JOC The Journal of Organic Chemistry

Article

pubs.acs.org/joc

Mechanisms of Lactone Hydrolysis in Acidic Conditions

Rafael Gómez-Bombarelli,[†] Emilio Calle,[‡] and Julio Casado*[,‡]

[†]Department of Physics, School of Engineering and Physical Sciences, Heriot-Watt University, EH14 4AS Edinburgh, U.K.

[‡]Departamento de Química Física, Universidad de Salamanca, Plaza de los Caídos 1-5, E-37008 Salamanca, Spain

Supporting Information

ABSTRACT: The acid-catalyzed hydrolysis of linear esters and lactones was studied using a hybrid supermolecule−polarizable continuum model (PCM) approach including up to six water molecules. The compounds studied included two linear esters, four β-lactones, two γ-lactones, and one δ-lactone: ethyl acetate, methyl formate, β-propiolactone, β-butyrolactone, β-isovalerolactone, diketene (4-methyleneoxetan-2-one), γ-butyrolactone, 2(5*H*)-furanone, and δ-valerolactone. The theoretical results are in good quantitative agreement with the experimental measurements reported in the literature and also in excellent qualitative agreement with long-held views regarding the nature of the hydrolysis mechanisms at molecular level. The present results help to understand the balance between the unimolecular ($A_{AC}1$) and bimolecular ($A_{AC}2$) reaction pathways. In contrast to the experimental setting, where one of the two branches is often occluded by the requirement of rather extreme experimental conditions, we have been able to estimate both contributions for all the compounds studied and found that a transition from $A_{AC}2$ to $A_{AC}1$ hydrolysis takes place as acidity increases. A parallel work addresses the neutral and base-catalyzed hydrolysis of lactones.

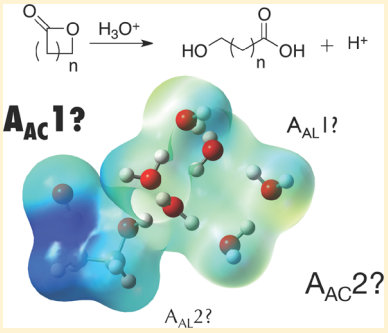

1. INTRODUCTION

As is also the case with neutral and base-catalyzed mechanisms, the acid-catalyzed hydrolysis of esters has seldom been the subject of computational approaches in comparison with the exceedingly large numbers of empirical works.[1] The somewhat similar hydrolysis of carboxylic acid derivatives such as amides has been studied more often[2−4] due to their relation with the peptide bond cleavage in proteins. In the case of lactone hydrolysis, the disproportion is even larger, computational works being especially scarce.

The existing mechanisms of acid-catalyzed ester hydrolysis can be seen as the counterparts of those of neutral hydrolysis, albeit involving the protonated ester, and are classified using the same system.[5] The increased electrophilicity of the protonated ester group results in a decrease in the energy barrier of reaction pathways that are not energetically available for the neutral species, such as the unimolecular acyl cleavage mechanism ($A_{AC}1$).[6] Furthermore, pre-equilibrium protonation results in an additional kinetic step that introduces further complexity in acid-catalyzed hydrolysis mechanisms.

At acidic pH, nonactivated esters usually favor the $A_{AC}2$ mechanism, whereas those species prone to giving off stable carbocations, such as tertiary alkyl esters, hydrolyze rapidly at low acid concentrations through the $A_{AL}1$ mechanism. $A_{AC}1$ is rare and is observed mostly for esters of very bulky acids or in strongly acidic media. In these highly concentrated solutions, the activity of water is very low, and carbon−oxygen bond cleavage occurs first, followed by elimination or by addition of a water molecule. The $A_{AL}2$ mechanism is very rare. In lactones, it has only been observed by using isotopic tracers in cases in which the competing hydrolysis through other mechanisms was reversible and using very harsh conditions.[7,8]

In this work, the mechanisms of hydrolysis of some lactones were studied. The compounds chosen (Scheme 1) were four β-lactones (β-propiolactone (BPL), β-butyrolactone (BBL), β-isovalerolactone (BIVL), and diketene (DIK)), two γ-lactones (γ-butyrolactone (GBL) and 2-furanone (FUR)), and one δ-lactone (δ-valerolactone (DVL)). For use as a reference for the lack of ring strain, and more importantly as a general model of linear ester reactivity, two linear esters whose hydrolysis has been widely studied were also included. The linear esters, ethyl acetate (AcOEt) and methyl formate (COOMe), have very

Scheme 1. Compounds Studied

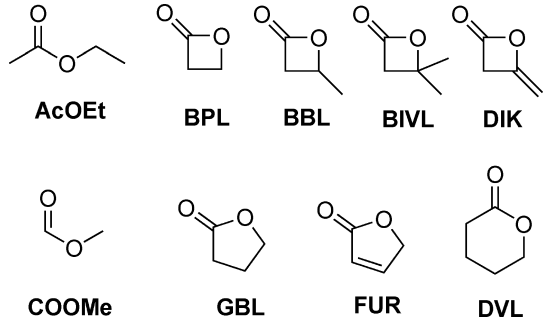

Received: February 4, 2013
Published: June 3, 2013

   dx.doi.org/10.1021/jo4002596 | J. Org. Chem. 2013, 78, 6880−6889

different reactivities; AcOEt is rather unreactive, and COOMe is very easily hydrolyzed.

A hybrid supermolecule−polarizable continuum model (PCM) approach with up to six water molecules was used to take into account the specific role of solvent molecules. Calculations were also carried out in systems with few or no water molecules in an attempt to model how hydrolysis mechanisms can change in media in which the activity of water is lowered.

2. COMPUTATIONAL DETAILS

2.1. Reaction Paths. Geometries were optimized at the DFT B3LYP/6-31++G(d,p) level of theory, using the default PCM solvent model with default parameters followed by harmonic analysis of the structures (zero imaginary vibration modes for minima and one for transition states). This level of theory has been used for similar systems such the hydration reaction of the carbonyl group[9] and produces results within less than 1 kcal of the larger 6-311++G(2df,2p) basis set. Different correlation−exchange functionals were also found to produce equal or worse results.

For species attracting most interest (e.g., those corresponding to the transition states of the rate-limiting steps and the corresponding minima), optimizations were refined at the DFT/6-311++G(2df,pd) level and were also followed by single-point energy calculations at the MP2/6-31++G(d,p), MP4/6-31++G(d,p), and QCISD/6-31++G(d,p) levels of theory.

Thermochemical values were computed at 298 K using uncorrected DFT B3LYP/6-31++G(d,p) frequencies. Intrinsic reaction coordinate (IRC) paths were computed to link transition states with the corresponding reactants and products. Atomic polar tensor (APT) charges were computed when necessary. All calculations were performed using Gaussian 09[10] on a Mountain workstation.

2.2. Δ*H* in Solution. Whereas PCM calculations include the contribution of solvation free energy to the total energy and thus afford Δ*G* with appropriate statistical thermodynamics and solvation terms, enthalpy values as reported by the software in PCM calculations include the statistical thermodynamics enthalpic term plus the solvation *free energy* contribution. Therefore, unlike G_{PCM}, H_{PCM} needs to be corrected for the difference between solvation enthalpies and free energies ($T\Delta S_{solv} = \Delta H_{solv} - \Delta G_{solv}$).

As Pliego and Riveros have discussed,[11] one can estimate absolute solvation enthalpies (and entropies) for ionic species from cluster-continuum calculations ($\Delta H^*_{solv}(ion)$) by combining the clustering enthalpy (or entropy) of the supermolecule, obtained through statistical mechanics ($\Delta H^\circ_{clust}(supermol)$), the vaporization enthalpy (or entropy) of the solvent ($\Delta H_{vap}(solvent)$), and the solvation enthalpy (or entropy) of the supermolecule ($\Delta H^*_{solv}(supermol)$) as shown in eqs 1 and 2 (the asterisk and degree symbol superscripts refer to 1 atm and 1 mol dm^{-3} standard states respectively).

$$\Delta H^*_{solv}(ion) = \Delta H^\circ_{clust}(supermol) + n\Delta H_{vap}(solvent) + \Delta H^*_{solv}(supermol) \quad (1)$$

$$\Delta S^*_{solv}(ion) = \Delta S^\circ_{clust}(supermol) + n\Delta S_{vap}(solvent) + \Delta S^*_{solv}(supermol) \quad (2)$$

Of these three contributions, the third term is unavailable from PCM calculations, but it can be estimated according to the Born model from the PCM solvation free energy and the temperature dependence of the solvent relative permittivity, ε.[11]

$$\Delta H^*_{solv}(supermol) = \Delta G^*_{solv}(supermol)\left(1 - \frac{T}{\varepsilon - 1}\frac{\partial \ln \varepsilon}{\partial T}\right) \quad (3)$$

$$\Delta S^*_{solv}(supermol) = -\Delta G^*_{solv}(supermol)\left(\frac{1}{\varepsilon - 1}\frac{\partial \ln \varepsilon}{\partial T}\right) \quad (4)$$

It should be noted that when modeling reaction pathways, we are interested in variations of *G*, *H*, and *S* along the path within solution rather than absolute changes from gas phase to solution, and thus only $\Delta\Delta H^*_{solv}$ and $\Delta\Delta S^*_{solv}$ along the path are required.

$$\Delta\Delta H^*_{solv}(ion) = \Delta\Delta H^\circ_{clust}(supermol) + \Delta\Delta H^*_{solv}(supermol) \quad (5)$$

$$\Delta\Delta S^*_{solv}(ion) = \Delta\Delta S^\circ_{clust}(supermol) + \Delta\Delta S^*_{solv}(supermol) \quad (6)$$

$\Delta\Delta G^\circ_{clust}$, $\Delta\Delta H^\circ_{clust}$, and $\Delta\Delta S^\circ_{clust}$ contributions are fully taken into account in supermolecule−PCM calculations through the statistical thermodynamics terms, and hence the only term we need to correct for is the difference $T\Delta\Delta S^*_{solv}(supermol) = \Delta\Delta H^*_{solv}(supermol) - \Delta\Delta G^*_{solv}(supermol)$, which is unaccounted in PCM calculations. Activation enthalpies were thus computed using the thermal enthalpies at 298 K as reported by the software in PCM calculations and were corrected by adding the $T\Delta\Delta S^*_{solv}(supermol)$ from eq 4. ΔG^*_{solv} values were estimated as the difference in single point energy between gas-phase and PCM calculations, using using the IEFPCM solvation model in the SMD parametrization.[12] We have used $(\partial \ln \varepsilon)/\partial T = -4.57 \times 10^{-3}$ K^{-1} and $\varepsilon = 78.4$ at 298 K.[13]

$$\Delta H = \Delta H_{PCM} + T\Delta\Delta S^*_{solv}(supermol) \quad (7)$$

2.3. Acid Dissociation Constants. The computational determination of equilibrium constants in solution is a demanding task, since the thermodynamic definition of *K* (eq 8) implies that an uncertainty of only ∼5 kJ mol^{-1} will result in an error of 1 log units in pK_a and thus a 10-fold error in the equilibrium constant.

$$\ln K = \frac{-\Delta G^\circ}{RT} \quad (8)$$

Whereas gas-phase reaction free energies can be computed with very good accuracy (1 kcal/mol), errors in solvation energies from polarizable continuum models are usually several fold larger, especially in the case of ions. Since the acid dissociation reaction is highly unsymmetrical in terms of solvation, systematic errors of several log units may arise from the inaccuracies in solvation energies. Moreover, calculation of the hydration energy of the proton is difficult and a certain controversy exists about which reference value, either empirical or theoretical, is preferable. The most common solutions for these handicaps include the use of thermodynamic cycles, together with explicit solvent molecules to better account for specific solvent−solute interactions, or the use of a relative or proton-exchange approach to correct systematic errors by means of a homodesmic reaction. The existing approaches and their (dis)advantages, together with a detailed consideration of the thermodynamic standard states in these thermodynamic cycles, have been reviewed in depth[14] and thus will only be described briefly.

In the absolute approach, ΔG°_{prot} is calculated as the reaction free energy of eq 9 ($\Delta G^\circ_{prot} = G^{sol}_{H^+} + G^{sol}_{A} - G^{sol}_{AH^+}$) using computational estimates for $G^{sol}_{A^-}$ and G^{sol}_{AH}, together with the free energy of the proton in aqueous solution. The value $G^{sol}_{H^+} = -1129.8$ kJ mol^{-1} was used, as suggested by Ho and Coote,[14] and includes the free energy of the proton in the gas phase (−26.25 kJ mol^{-1})[15] and its free energy of solvation with respect to a standard state of 1 mol dm^{-3} (−1111.46 kJ mol^{-1}).[16−18] In addition, since the number of moles on each side of the chemical equation is different, a thermodynamic correction of +*RT* ln *RT* (+7.92 kJ mol^{-1}) needs to be included to go from the 1 atm standard state of gas-phase free energies to the 1 mol dm^{-3} standard state of calculations in solution.

$$AH^+_{sol} \rightleftharpoons A_{sol} + H^+_{sol} \quad (9)$$

The free energy in solution for each species (G^{sol}_i) is computed as the sum of gas-phase free energy, G^{gas}_i, calculated using a high-level method, plus free energy of solvation (ΔG^{sol}_i). ΔG^{sol}_i is usually taken as the difference in energy between gas-phase and PCM calculations using a lower level of theory consistent with the parametrization of the solvent in the particular PCM model of choice. This can be done using both gas-phase and solution equilibrium geometries, to account for the

dx.doi.org/10.1021/jo4002596 | J. Org. Chem. 2013, 78, 6880−6889

geometrical relaxation upon solvation. It has recently been pointed that gas-phase calculations may be avoided completely since results obtained using high-level methods combined with PCM solvation have similar accuracy.[19]

In the proton-exchange (PE) scheme, the acid dissociation free energy is computed from the reaction free energy of eq 10 ($pK_a = \Delta G^{\circ}_{PE}/(RT \ln 10) + pK_a(BH^+)$). This gives much more accurate results due to favorable error cancellation in the solvation energies. The accuracy of this approach depends mainly on the experimental accuracy in the experimentally known $pK_a(BH^+)$ and the similarity between BH and AH.

$$AH^+ + B \rightleftharpoons A + BH^+ \quad (10)$$

In this work, we opted for a proton-exchange or relative method (eq 10), using acetyl acetate as a reference ($pK_a = -3.90 \pm 0.03$[20]) and also included the absolute method for comparison. We have used the compound method CBS-QB3[21,22] for gas-phase free energies and B3LYP/6-31+G(d) for the solvation free energies, using the IEFPCM solvation model in the SMD parametrization.[12] ΔG_i^{sol} was computed as the difference in energy between the aqueous-phase energy of the solution equilibrium geometry and the gas-phase energy of the gas equilibrium geometry. A very similar approach has been successfully applied in a study of the α-carbon acidity of lactones and cycloketones.[23]

3. RESULTS AND DISCUSSION

As is often the case, β-lactones are an example of particular behavior and also of the large mechanistic influence of small changes in structure. Unlike unactivated linear esters, such as ethyl acetate, which require concentrations exceeding 90% of mineral acid for the $A_{AC}1$ mechanism to be observed,[24,25] BPL,[26] BBL,[27,28] and DIK[29] are known to follow the $A_{AC}1$ mechanism under relatively milder conditions (20% H_2SO_4) in which water is more abundant. The tertiary alkyl nature of the alkyl-oxygen carbon in BIVL governs its reactivity in acidic media, and it thus provides an example of the $A_{AL}1$ mechanism. Larger primary lactones (GBL, FUR, and DVL) and linear esters (AcOEt and COOMe) follow the $A_{AC}2$ pathway.

3.1. Basicity of Esters. Since the protonation of the carbonyl oxygen precedes any reaction in all the proposed reaction schemes, the determination of the acid dissociation constants of protonated esters is of interest and was investigated first.

Esters are weak bases that only undergo protonation in strongly acidic media, and hence their pK_a values have been defined in the literature in terms of Hammett's acidity function, thus assuming that the acidity function for esters is linear with respect to H_0. Esters, however, are not well-behaved Hammett bases,[6] and more rigorous approaches have been used, such as Bunnett and Olsen's correction for nonlinearity between acidity functions or development of a new acidity function *de novo*.[30]

In general, alkyl esters have very similar acid dissociation constants, with very early experiments proposing acidity constants around a standard value of $pK_a(AcOEt) = -7.0$.[31,32] More modern works using NMR measurements give values of $pK_a(AcOEt) = -3.5 \pm 0.3$,[30] with moderate variation for other simple alkyl aliphatic chains. Very similar results were also obtained using UV-titration, $pK_a(AcOEt) = -3.0$ to -3.3.[30] These estimates have been confirmed more recently using ^{13}C NMR spectroscopy $pK_a(AcOEt) = -3.90 \pm 0.03$,[20] and we have used this value for the proton-exchange calculations.

The protonation pre-equilibrium is quite important as regards acid-catalyzed hydrolysis, and variations in reactivity can sometimes be explained by differences in the protonation free energy. For instance, esters with electron-withdrawing substituents, such as haloesters, are weakly basic and show little acid catalysis. Also, the contribution of this initial step to the overall entropy and enthalpy of activation is not known, since the experimental activation parameters are measured for the global reaction.

Although great steps have been taken in the last years in the form of ingenious thermodynamic cycles and high-level calculations, the accurate (i.e., within ± 1 pK unit) prediction of acid dissociation constants *in silico* for any class of molecules is still a formidable challenge.[14] In addition to the well-known difficulties of how to describe solvation of very different species (ions vs neutral species), esters are extremely weak bases, so much so that the levels of theory used in this work predict that the protonated carbonyl ester is not a minimum in the potential energy surface when surrounded by an explicit solvation shell. Therefore unconstrained geometry optimization at the MP2 and B3LYP levels of theory with a range of basis sets in implicit solvent leads to proton transfer from the carbonyl oxygen to the surrounding hydration shell.

This is in contrast with the experimental evidence, which clearly suggests that protonated carbonyl esters are actual intermediates that exist physically, at least in the strongly acidic solutions used to determine their acid dissociation constants, in which water has very low activity. In addition, the mechanistic analysis of kinetic evidence such as the rather low activation entropies,[6] suggests that the protonated carbonyl is a physical intermediate in pre-equilibrium with the reactants. Thus, we have performed calculations only in implicit solvent.

The values obtained for the gas-phase dissociation free energy (ΔG^{gas}_{prot}), the difference in solvation free energy between AH^+ and A ($\Delta\Delta G^{sol} = \Delta G^{sol}_{A} - \Delta G^{sol}_{AH^+}$) and the absolute and relative pK_a values are reported in Table 1.

Table 1. Energies of Dissociation and pK_a of the Esters Studied with AcOEt as a Reference ($pK_a = -3.9$[20])

	$-\Delta G^{gas}_{prot}$ (kJ mol^{-1})	$\Delta\Delta G^{sol}$ (kJ mol^{-1})	$-pK_a$ absolute	$-pK_a$ relative
COOMe	771.9	274.0	11.5	5.7
AcOEt	822.4	239.8	8.6	ref
BPL	782.6	250.6	13.7	9.0
BBL	800.7	236.6	13.0	8.3
BIVL	815.6	225.2	12.4	7.6
DIK	765.9	248.4	17.0	12.3
GBL	828.6	228.3	9.6	4.8
FUR	820.8	238.6	9.1	4.4
DVL	859.0	213.2	6.9	2.1

The comparison of the theoretical estimation for AcOEt with the experimental value of -3.90 shows that the absolute approach affords results with large systematic errors for the protonation reaction of esters and underlines the need to use a relative or proton-exchange method. In good agreement with the literature, relative trends within the studied compounds suggest that the basicity decreases (lower pK_a values) as the inherent reactivity increases: the more electrophilic the ester carbon, the smaller the negative partial charge on the acyl oxygen and thus the lower the basicity. As regards the β-lactones, this decreased basicity has been studied both theoretically and empirically in the gas phase and has been attributed to the lower sp^2 character of the ester carbon in four-membered lactones.[33] The electron-donating effect of sub-

dx.doi.org/10.1021/jo4002596 | J. Org. Chem. 2013, 78, 6880−6889

Scheme 2. $A_{AL}1$, $A_{AC}1$, and $A_{AL}2$ Mechanisms of Neutral Hydrolysis

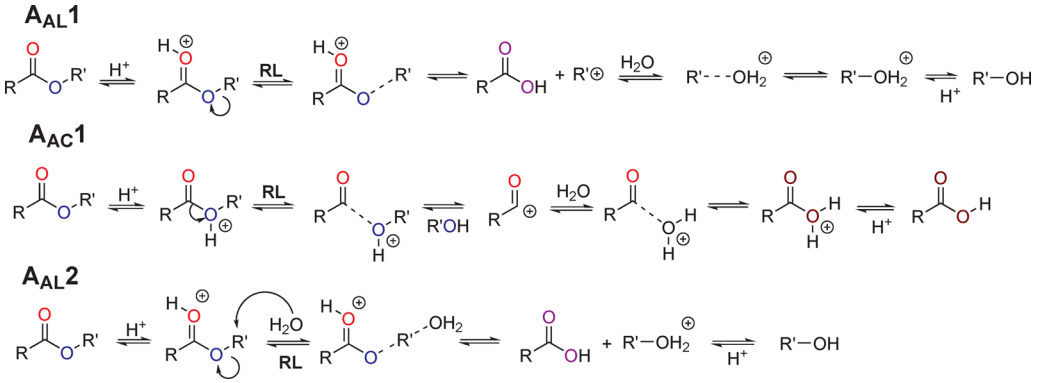

Table 2. Energy Barriers for the Rate-Limiting Step in the Mechanisms of Acid-Catalyzed Lactone Hydrolysis

	ΔH (kJ mol^{-1})				ΔG (25 °C) (kJ mol^{-1})			
	$A_{AL}2$	$A_{AL}1$	$A_{AC}1$	$A_{AC}2$	$A_{AL}2$	$A_{AL}1$	$A_{AC}1$	$A_{AC}2$
COOMe	183.2	257.4	231.6	85.7	164.3	245.7	228.9	93.6
AcOEt	186.4	227.8	182.3	96.0	171.3	204.3	177.8	114.3
BPL	119.7	190.4	101.9	95.4	108.8	192.1	103.0	98.1
BBL	109.5	126.6	105.3	94.8	119.4	113.6	111.2	98.5
BIVL	N/A	89.0	112.5	97.1	N/A	70.7	123.8	101.1
DIK	N/A	165.4	85.4	88.5	N/A	145.6	92.2	93.0
GBL	128.9	204.1	189.2	87.1	123.6	179.2	173.6	86.6
FUR	142.9	224.3	183.1	104.9	145.9	200.4	167.0	112.1
DVL	150.9	172.5	170.4	73.7	145.0	171.8	182.2	83.6

stituentes in the ring increases the basicity of the β-lactones, as observed in the BPL−BBL−BIVL series. COOMe is a weaker base, due to the lack of electron-donating alkyl substituents. The γ lactones are approximately as acidic as AcOEt, whereas DVL is significantly more basic, in keeping with its increased reactivity in acidic medium with respect to GBL.[34]

When attempting to estimate the basicity of the alkyl oxygen, we found that the protonated ester is not a minimum not only regarding proton transfer to the solvent but also regarding ring cleavage (as in the $A_{AC}1$ hydrolysis), and thus estimates cannot be given for alkyl-oxygen basicity.

The fact that protonated esters in a solvent cluster are not minima in the potential energy surface at the DFT-B3LYP and MP2 levels of theory potentially has very important implications; for instance, it means that the acid-catalyzed transition states correspond to general acid catalysis by hydronium ions rather than reactions by a protonated intermediate in equilibrium with the reactants (see below). However, further work using high-level *ab initio* methods beyond DFT will be needed to analyze how the delicate interplay between level of theory and implicit and explicit solvation influences these results and whether they can be related to experimental conditions with high and low water activity.

3.2. Reactant complex. Finding global minimum structures for solvated structures using a cluster-continuum approach is challenging since many possible arrangements for the explicit solvent molecules are possible and even if only a few solvent molecules are present, this parameter space soon becomes too vast to explore. Aqueous solution is particularly arduous, given both the directionality of hydrogen bonding and the high energies involved for these noncovalent interactions. Organic molecules such as esters require additional efforts, since they feature two oxygen atoms that can interact with the solvent through hydrogen bonds. This interaction is usually weaker than the one among water molecules, and hence minima may be located, corresponding to highly bound water clusters that show very little interaction with the solute. If not enough explicit molecules are present in the solvation shell to maintain this level of solvent−solvent interactions along the reaction path under study, this may result in spurious (de)stabilization of certain intermediate species.

Often in the literature, IRC calculations are used to find the reactant and product complexes that each particular transition state connects, and these are taken to be in great proximity to the true global minima. Whereas this avoids a toilsome search and the possibility of finding unrealistic minima featuring strong solvent−solvent interactions that are not featured in the transition state due to the limited number of solvent molecules present, it also can lead to overestimations of the reactant energy.

Since various, very different reaction paths are studied in this work, we have analyzed the ones reached from the different IRC calculations and also tested additional solvent arrangements by hand and have chosen the one showing the lowest free energy. Whereas the free energy differences among the minima considered were small (<5 kJ mol^{-1}), this choice has some effect in the absolute prediction (see below) but none in the mechanistic diagnosis.

3.3. $A_{AL}1$, $A_{AC}1$ and $A_{AL}2$ mechanisms. The $A_{AL}1$, $A_{AC}1$, and $A_{AL}2$ mechanisms are simple and are thought to take place in a single, rate-limiting step, excluding fast proton transfers and rapid addition of water to carbocations or eliminations (Scheme 2). The more common $A_{AC}2$ is more complex and will be discussed separately (see below).

dx.doi.org/10.1021/jo4002596 | J. Org. Chem. 2013, 78, 6880−6889

For ease of comparison, Table 2 reports the enthalpy and free energy differences between the reactants and the transition state for the rate-limiting step for all the compounds and mechanisms studied. Since the cleavage step in the unimolecular mechanisms ($A_{AL}1$ and $A_{AC}1$) and the addition in the bimolecular $A_{AC}2$ pathway preclude any further reaction, a high barrier blocks the entire pathway, and thus only this step was included in this comparison, even if this is step is not ultimately rate-limiting within its pathway. In analogy with the experimental situation, the water + hydronium + ester cluster (Figure 1) was chosen as a reactant, rather than the protonated ester, such that the inherent basicity of each ester was taken into account.

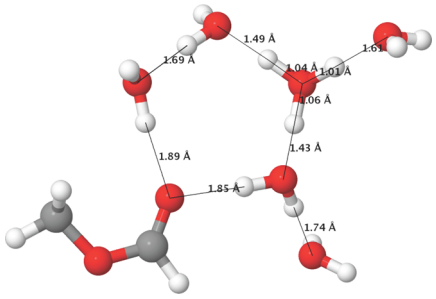

Figure 1. Equilibrium geometry for the encounter complex of COOMe, H_3O^+, and five solvent molecules.

In summary, only the tertiary BIVL favored $A_{AL}1$. The *β*-lactones BPL and DIK showed similarly low barriers for the $A_{AC}1$ and $A_{AC}2$ mechanisms, whereas BBL favors $A_{AC}2$ by a small margin (Figure 2). The larger lactones and the linear esters follow the usual $A_{AC}2$ pathway.

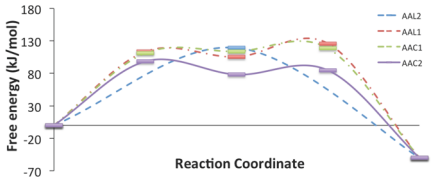

Figure 2. Variation in the free energy (25 °C) along the various reaction paths for the acid hydrolysis of BBL.

$A_{AL}2$ was disfavored for all the compounds, in keeping with the fact that, experimentally, it has never been observed to be predominant. As occurred in neutral hydrolysis, no transition states could be located for the bimolecular alkyl cleavage of BIVL and DIK. Also, in a similar fashion to what occurred with the neutral $B_{AL}2$ mechanism, the activation entropies for $A_{AL}2$ were quite high, even positive in some cases, whereas, in analogy with the neutral counterpart, small negative values would be expected.

3.3.1. The $A_{AL}1$ Mechanism. Table 3 reports the enthalpy and free energy differences between the reactants and transition states and intermediate species in the reaction path for the $A_{AL}1$ mechanism. Since the reaction products following the unimolecular cleavage (TS_{CLV}) are carbocations that may undergo further reactions, such as elimination or addition of a water molecule, we included the carbocation (CAT) and the transition state corresponding to the attack of water (TS_{AD}) and elimination (TS_{EL}) in cases for which this mechanism shows higher availability.

The $A_{AL}1$ reaction has positive activation entropies, in keeping with the fact that one bond is broken and none are formed. Interestingly, both the addition of water to the carbocation and elimination to afford an unsaturated ester had barriers (with reference to the reactants as starting point) that are somewhat higher than that of the unimolecular cleavage itself, which makes the step kinetically rate-limiting. However, some other unexplored mechanisms may provide faster decomposition alternatives, especially in experimental conditions where buffer species or dissociated mineral acids may play an important role.

The stabilizing effect of the substituent on the alkyl carbon from primary to tertiary is evident in the BPL−BBL−BIVL series.

$A_{AL}1$ is observed in the hydrolysis of esters whose leaving group is capable of yielding stable carbocations, and thus mainly for esters of tertiary alcohols, such as *tert*-butyl acetates. Among the compounds of choice, BIVL (Figure 3) is the only one that clearly (more than 30 kJ mol^{-1}) favors this $A_{AL}1$ over the alternatives (Table 2).

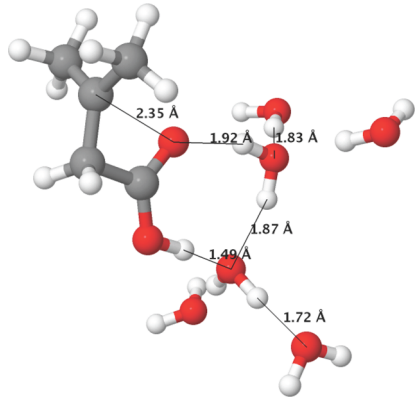

Figure 3. Equilibrium geometry for the $A_{AL}1$ transition state for BIVL.

3.3.2. The $A_{AC}1$ Mechanism. The values reported in Table 4 show very high theoretical energy barriers for the $A_{AC}1$ cleavage of the linear esters that decrease with decreasing ring size in lactones. Activation enthalpies were very high, and the thermoentropic contributions were close to zero, in keeping with the unimolecular nature of the mechanism.

The species formed following the unimolecular carbon−oxygen bond cleavage (TS_{CLV}) were the corresponding acyl cations. Since these carbocations are intermediates that undergo addition of a water molecule, we included the

Table 3. Energy Barriers for the $A_{AL}1$ Acid Hydrolysis of Some Lactones

	ΔH (kJ mol^{-1})				ΔG (25 °C) (kJ mol^{-1})			
	TS_{CLV}	CAT	TS_{AD}	TS_{EL}	TS_{CLV}	CAT	TS_{AD}	TS_{EL}
BBL	126.6	122.5	126.8	100.7	113.6	102.4	126.0	103.8
BIVL	90.8	85.5	68.9	79.5	70.7	56.9	84.0	76.0

dx.doi.org/10.1021/jo4002596 | J. Org. Chem. 2013, 78, 6880−6889

Table 4. Energy Barriers for the $A_{AC}1$ Acid Hydrolysis of Some Lactones

	ΔH (kJ mol^{-1})			ΔG (25 °C) (kJ mol^{-1})		
	TS_{CLV}	CAT	TS_{AD}	TS_{CLV}	CAT	TS_{AD}
BPL	101.9	97.3	116.2	103.0	99.6	111.6
BBL	105.3	101.5	115.5	111.2	113.8	118.5
BIVL	112.5	109.5	124.7	123.8	126.4	129.5
DIK	85.4	77.6	94.8	92.2	82.6	100.3

carbocation (CAT) and the transition state corresponding to the attack of water (TS_{AD}) in cases for which this mechanism is lower in energy.

The acyl cation moiety was not hydrogen-bonded to its water hydration shell, and a lack of specific interactions with the solvent can be deduced from the large distance to the solvent molecules (Figure 4). Since they lay at such high energy, their

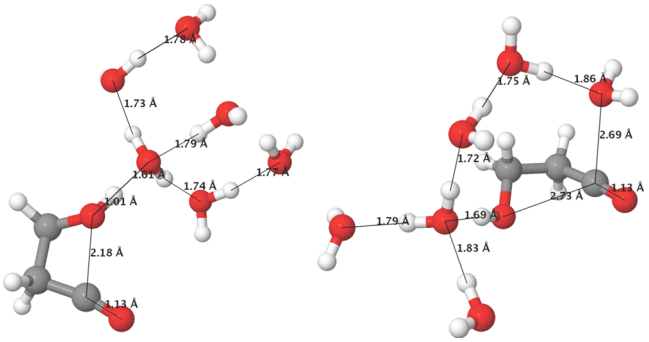

Figure 4. Structure of the $A_{AC}1$ cleavage transition state and its acyl cation product.

hydration step is predicted to be partially rate-limiting as regards the global progress of the reaction, although other unexplored mechanisms may provide faster decomposition alternatives.

3.4. The $A_{AC}2$ Mechanism. The $A_{AC}2$ mechanism is the most usual acid-catalyzed hydrolysis pathway. Like its neutral and base-catalyzed analogs, it takes place in two steps (Scheme 3): an addition reaction leads to the tetrahedral intermediate, which in turn decomposes. Whereas the breakdown kinetics of the intermediate has received less attention since this step is usually not rate-limiting, the addition step and the nature of the intermediate have attracted much discussion, especially regarding whether the reaction takes place by the base-catalyzed addition of water on the protonated carbonyl (which yields a neutral tetrahedral intermediate) or by the direct attack of water, affording a charged intermediate.

The calculated differences in free energy and enthalpy for the addition step (TS_{AD}), the intermediate (DIOL), the cleavage reaction (TS_{CLV}), and the single-step concerted reaction (TS_{UNI}) are reported in Table 5.

3.4.1. Addition. Rather than by direct addition (Scheme 4, AD.1), it has been suggested that the attack of a water molecule on the protonated carbonyl is base-catalyzed by an additional water molecule (Scheme 4, AD.2). Thus, the reaction would yield a unprotonated partially esterified orthoacid as the tetrahedral intermediate and a hydronium ion instead of the protonated orthoacid. The evidence for this proposed mechanism ranges from reaction symmetry (if the breakdown in the tetrahedral intermediate is acid-catalyzed, then the opposite must occur in the addition reaction) to the very high acidity of the protonated diol that is the tetrahedral intermediate.

The transition states found in this work correspond to such a mechanism featuring water as a general base catalyst (AD.2 in Scheme 4), and no uncatalyzed reaction was observed. Two molecules were observed to be involved in the rate-limiting step, in keeping with the empirical evidence suggesting that the acid hydrolysis of most esters under acidic conditions is second-order in water.[6]

As reported in Table 5, the β-lactones afforded relatively high barriers for this mechanism. This is possibly related to the low basicity of their carbonyl oxygen, which is the required protonation site for this mechanism. The free energy barriers were quite high for FUR and AcOEt, in keeping with their low general reactivity, whereas COOMe, and especially GBL (Figure 5) and DVL, are higly reactive.

3.4.2. Intermediate. The tetrahedral intermediates formed (DIOL in Table 5) can be seen as partially esterified orthoacids. As occurs in neutral and alkaline hydrolyses, these species lay at a fairly high energy, with the exception of DIK. This is due to the presence of two methylene carbons in the ring of DIK: the square geometry of β-lactones enforces 90° angles, and DIK has two sp^2 carbon atoms, whose preferred bond angle is 120°. Transition of the sp^2 carbonyl carbon to sp^3 hybridization is thus especially favored in DIK.

3.4.3. Cleavage. The breakdown transition states were symmetrical to those for the addition reaction and feature a hydronium-catalyzed cleavage step (Scheme 5, CLV.2) rather than a concerted mechanism (Scheme 5, CLV.1). This is in agreement with recent results for the hydrolysis of COOMe using a large number of water molecules (up to 15) in the hydration shell.[1]

For the larger lactones and the linear compounds, the cleavage step is kinetically significant, since the barrier for the breakdown is very similar to that for the addition. This is more evident for haloesters, which are very weak bases that are not protonated even in 100% sulfuric acid. In general, haloesters do not undergo significant acid-catalyzed hydrolysis, compared with fast $B_{AC}2$ hydrolysis, since the $A_{AC}2$ pathway is blocked by the low pK_a values, although general acid catalysis is still possible. Interestingly, the hydrolysis rate of haloesters with poorer leaving groups is increased in acidic medium. Since the $B_{AC}2$ and $A_{AC}2$ mechanisms share the tetrahedral intermediate, this can interpreted as a switch from a $B_{AC}2$ (co)rate-limiting cleavage step to an $A_{AC}2$ acid-catalyzed cleavage, even if the addition step is insensitive to the acid catalyst because of the low basicity of the ester group.

3.4.4. Single-Step Hydrolysis. As was the case in the neutral mechanism, a single-step hydrolysis mechanism was also observed (TS_{UNI}), in which nucleophilic addition, acyl-oxygen cleavage, and protonation of the alkyl oxygen by a hydronium

Scheme 3. $A_{AC}2$ Mechanism of Ester Hydrolysis

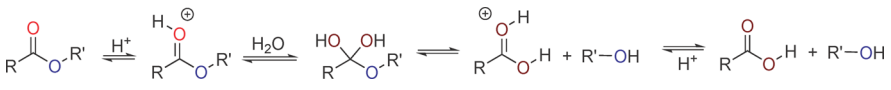

dx.doi.org/10.1021/jo4002596 | J. Org. Chem. 2013, 78, 6880–6889

Table 5. Energy Barriers for the $A_{AC}2$ Hydrolysis of Some Lactones

	ΔH (kJ mol^{-1})				ΔG (25 °C) (kJ mol^{-1})			
	TS_{AD}	DIOL	TS_{CLV}	TS_{UNI}	TS_{AD}	DIOL	TS_{CLV}	TS_{UNI}
COOMe	85.7	62.5	77.1	152.6	93.6	80.3	88.1	161.9
AcOEt	96.0	79.0	103.6	166.1	114.3	107.7	106.7	171.7
BPL	95.4	62.0	60.6	122.6	98.1	75.0	77.3	123.2
BBL	94.8	65.5	62.3	128.8	98.5	78.2	84.7	131.2
BIVL	97.1	66.3	68.7	133.4	101.1	77.1	88.8	135.4
DIK	88.5	38.1	42.2	118.2	93.0	50.7	63.8	115.0
GBL	87.1	69.8	82.1	142.1	86.6	73.3	89.0	139.1
FUR	104.9	88.2	100.3	162.5	112.1	92.9	114.5	162.8
DVL	73.7	63.4	68.0	143.1	83.6	79.7	89.9	153.6

Scheme 4. Possible Addition Steps in the $A_{AC}2$ Hydrolysis Mechanism

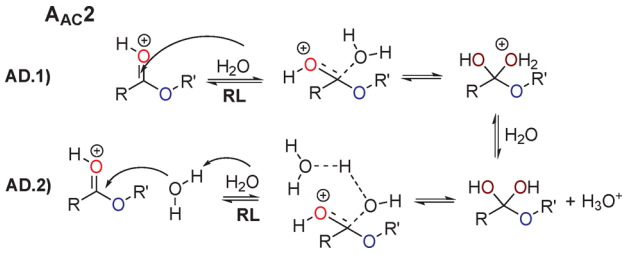

Scheme 5. Observed Cleavage Steps in the $A_{AC}2$ Hydrolysis Mechanisms

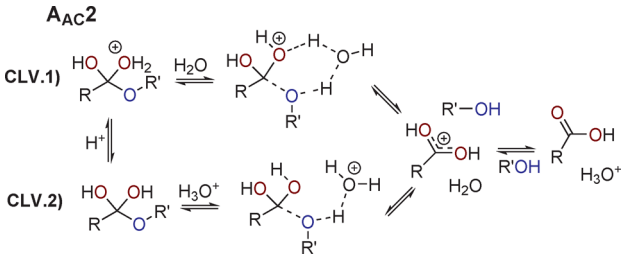

ion take place simultaneously. This pathway can be seen as an acid-catalyzed version of the fully concerted single-step neutral hydrolysis mechanism (designated TS_{UNI} in the parallel work dealing with neutral and base-catalyzed hydrolyses). This is, together with the $A_{AC}1$ mechanism, the only pathway we have found featuring alkyl-oxygen protonation, although this occurs synchronically with formation of a partial negative charge on the oxygen atom during C−O bond cleavage. This is in keeping with the very low basicity of the alkyl oxygen (see above). This reaction path is higher in energy than the catalyzed addition (Table 2) by about 25 kJ mol^{-1} in the case of the more strained compounds and up to 70 kJ mol^{-1} in the case of the linear esters and the larger lactone.

3.5. Comparison with the Experimental Results. Table 6 reports the actual hydrolysis mechanism for each compound, as deduced from experiments, and the pathway predicted to be most favored by the theoretical approach used in this work. The experimental and theoretical activation parameters, when available, are also reported. Experimental activation parameters for acid-catalyzed hydrolysis reactions were computed from the catalytic term, k_H/K_a, and thus include the contribution of both the protonation pre-equilibrium and the rate-limiting step. For consistency, the values reported in Table 6 are referred to the unprotonated reactants (hydronium + water cluster + ester). Whereas our results suggest that the cleavage step in the unimolecular pathways ($A_{AC}1$ and $A_{AL}1$, see above) may not the rate-limiting step since the subsequent addition/elimination steps are also significant, it is not clear whether this conclusion extrapolates to experimental conditions, and thus we report the barrier for the initial unimolecular cleavage.

3.5.1. Preferred Mechanism. In general, the results are in good qualitative agreement with the experimental mechanisms: no esters are known to follow the $A_{AL}2$ mechanism, which was disfavored in all the cases studied; linear esters and larger lactones are correctly predicted to follow the $A_{AC}2$ mechanism, and BIVL is hydrolyzed by the $A_{AL}1$ pathway.

The behavior of the other β-lactones, which experimentally follow the $A_{AC}1$ pathway, is more complex. The $A_{AC}1$ and $A_{AC}2$ hydrolyses are predicted to have very similar barriers, with differences ranging from −1 to +12 kJ mol^{-1}). This can be reconciled with the fact that most kinetic evidence points in the direction of, mostly, pure $A_{AC}1$ if the influence of the availability of water molecules is taken into account (see below).

Experimental work reported in the literature shows that the $A_{AL}1$ reaction is very sensitive to the dielectric constant of the medium, and its rate is decreased in media with organic cosolvent, sometimes to such a point that the mechanism switches to the standard $A_{AC}2$, which is slower in more polar media. This is consistent with the highly charged transition states found for $A_{AL}1$ hydrolysis, with computed electric dipole

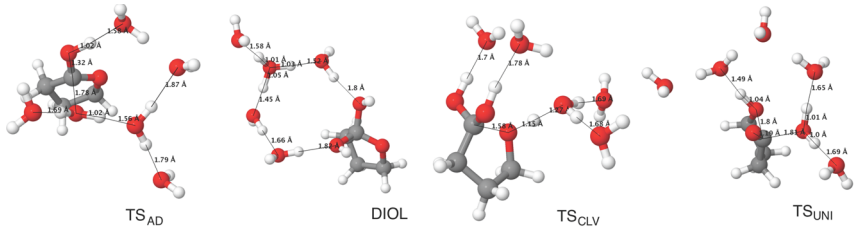

Figure 5. Equilibrium geometries for TS_{AD}, DIOL, TS_{CLV}, and TS_{UNI} in the $A_{AC}2$ mechanism for GBL.

dx.doi.org/10.1021/jo4002596 | J. Org. Chem. 2013, 78, 6880−6889

Table 6. Comparison of the Experimental and Theoretical Activation Parameters for the Acid Hydrolysis of the Compounds Studied

	$\Delta^{\ddagger}H°$ (kJ mol^{-1})		$\Delta^{\ddagger}S°$ (J mol^{-1} K^{-1})		$\Delta^{\ddagger}G°$ (25 °C) (kJ mol^{-1})		mechanism	
	exptl	calcd	exptl	calcd	exptl	calcd	exptl	calcd
COOMe	60 ± 2	86	−89 ± 7	−25	87 ± 3	94	$A_{AC}2$	$A_{AC}2$
AcOEt[35]	68 ± 1	96	−94 ± 1	−58	96 ± 1	114	$A_{AC}2$	$A_{AC}2$
BPL[26]		95/102		−11/−20	∼103	98/103	$A_{AC}1$	$A_{AC}2/A_{AC}1$
BBL[28]		95/105		−19/−30	∼105	99/111	$A_{AC}1$	$A_{AC}2/A_{AC}1$
BIVL[36]		91		36	∼88	81	$A_{AL}1$	$A_{AL}1$
DIK[29]		88/85		−15/−22	∼96	93/92	$A_{AC}1$	$A_{AC}2/A_{AC}1$
GBL[34]	65 ± 1	87	−96 ± 3	−3	94 ± 2	87	$A_{AC}2$	$A_{AC}2$
FUR		105		−27		112	$A_{AC}2$	$A_{AC}2$
DVL[34]	47 ± 1	74	−113 ± 5	−37	81 ± 2	84	$A_{AC}2$	$A_{AC}2$

moments around 20 D, compared with the much lower values for the alternative $A_{AC}2$ addition (around 5−6 D).

The theoretical structures of the acyl cations are in good agreement with the general crystallographic values for this functional group: a C−C bond at around 140 pm and a C≡O at about 110 pm[37,38] (Figure 4).

The solvent kinetic isotope effect (SKIE) reported in the literature for the $A_{AC}2$ mechanism is around $k_H/k_D \approx 0.6$. This inverse SKIE is in keeping with a mechanism preceded by a protonation pre-equilibrium such as the pathway proposed here. We have determined theoretical SKIE values for COOMe, GBL, and DVL of 0.66, 0.73, and 0.27, respectively, in good agreement with the experimental values of 0.77, 0.67, and 0.41.

3.5.2. Accuracy. The calculated relative pK_a values for the esters are in reasonable agreement with the values for alkyl esters. In addition, the values obtained for the lactones can shed some light on the reactivity of these compounds. Of the three ring sizes studied, the β-lactones are the least sensitive to acid catalysis, and very high acid concentrations are usually needed to observe an increase in the reaction rate. At the opposite extreme are the γ- and δ-lactones, which react readily in mildly acidic media. This can be partially explained in terms of their acid dissociation constants: the higher the acidity, the lower the concentration of the highly reactive protonated ester and hence the lower the catalytic effect of hydronium ions.

Regarding the activation parameters, the free energies show errors from −7 to +15 kJ mol^{-1} (the mean unsigned error is 7 kJ mol^{-1}). Whereas they are reasonably accurate when considering the diversity of the studied mechanisms, our results are insufficient to predict reaction rates within the so-called chemical accuracy (±1 kcal mol^{-1}). All the more, the reactant configuration used as a free energy reference corresponds to an encounter complex between a hydronium ion, the ester, and five water molecules and is in all likelihood higher in energy than the standard states of 1 mol dm^{-3} concentration for protons and ester and unit activity for water. Thus, all the reported results are expected to somewhat underestimate the theoretical activation free energy. Quantifying the free energy cost of forming the reactant complex from the ester and H_3O^+ at 1 mol dm^{-3} concentration is not a straightforward calculation.

Corrections have been carried out to take into account the role of solvation entropies of the supermolecule and improve PCM estimations of ΔH by adding a thermoentropic contribution, $T\Delta\Delta S^*_{solv}$(supermol). Since most entropic effects arise within the first solvation shell ($\Delta\Delta S^\circ_{clust}$(supermol)) and are well modeled with the statitiscal thermodynamic terms from the quantum chemistry calculations, ΔS^*_{solv}(supermol) is fairly constant for all reactant and transition state assemblies, and the thermoentropic corrections to ΔH are very small with values within ±2 kJ mol^{-1} (See Supporting Information). Activation enthalpies, in the few cases where experimental values are available for comparison, show large positive errors of which the origin is unclear.

The use of the larger 6-311+G(2df,pd) basis set did not result in a clear improvement in the activation free energies (the mean unsigned error is 7 kJ mol^{-1}, see Supporting Information) The post-HF single point energies (MP2/6-31++G(d,p), MP4/6-31++G(d,p), and QCISD/6-31++G(d,p)) on DFT-B3LYP/6-31++G(d,p) geometries afforded poor results (see Supporting Information). This is possibly due to the strong dependence of hydrogen-bond lengths and energies on the level of theory and the basis set used. The increased accuracy of the higher levels of theory is lost in the error induced by using DFT-B3LYP/6-31++G(d,p) geometries.

3.6. Hydrolysis in Strongly Acidic Media. Because of the electronic effects involved, the increased reactivity of activated esters is more evident in neutral hydrolysis mechanisms, milder in alkaline reactions, and much weaker in acid-catalyzed reactions. Therefore, acid hydrolysis is by far the least sensitive to increases in inherent reactivity.[6] As a consequence, in the experimental study of the hydrolysis of activated esters high concentrations of acid are needed in order to accelerate the acid-catalyzed reaction to a point where it is faster than the much enhanced neutral reaction.

The $A_{AC}2$ reaction requires the simultaneous availability of several water molecules: the nucleophile, the base catalyst, and those necessary for solvating the hydronium ion formed. By contrast, the $A_{AC}1$ transition state is unimolecular and shows little interaction with the surrounding water molecules. As a result, the $A_{AC}2$ pathway is disfavored in situations where few water molecules are present, whereas the contribution of the $A_{AC}1$ mechanism is less affected, since water does not play a significant role in the limiting steps other than generic hydration. It is not unexpected, then, for the $A_{AC}2/A_{AC}1$ ratio to fall as the concentration of acid increases and water becomes more scarce.

This is precisely what has been reported in the literature: the hydrolysis of primary and secondary alkyl esters in very concentrated acid solutions switches from the standard $A_{AC}2$ mechanism to $A_{AC}1$ when the concentration of mineral acid reaches 70−80% and few water molecules are available to simultaneously hydrate the ester and assist the rate-limiting nucleophilic attack.

Accordingly, the discrepancy between the predicted coexistence of $A_{AC}2$ and $A_{AC}1$ mechanisms in the hydrolysis of the

dx.doi.org/10.1021/jo4002596 | J. Org. Chem. 2013, 78, 6880−6889

Table 7. Energy Barriers for the Hydrolysis of Some Lactones with Few Water Molecules

	ΔG (25 °C) (kJ mol^{-1})							
	one solvent H_2O				minimal H_2O			
	$A_{AL}1$	$A_{AC}1$	$A_{AL}2$	$A_{AC}2$	$A_{AL}1$	$A_{AC}1$	$A_{AL}2$	$A_{AC}2$
COOMe	210.6	184.1	112.5	99.1	221.6	159.0	117.7	108.7
AcOEt	113.7	142.4	117.1	117.2	112.7	88.1	115.9	126.4
BPL	101.9	51.4	68.0	92.8	88.3	42.6	87.6	207.4
BBL	60.2	45.7	50.9	79.8	39.0	38.3	80.3	210.3
BIVL	22.6	58.2	64.3	89.0	7.2	49.0	51.0	211.7
DIK	88.0	17.4		68.3	61.8	35.4		209.3
GBL	158.6	107.0	112.1	105.9	154.1	77.4	119.0	215.8
FUR	180.8	113.4	130.0	139.7	222.4	103.5	141.6	241.0
DVL	149.0	107.8	132.4	109.6	123.0	85.4	118.3	218.2

β-lactones can be understood in the same terms. The acid-catalyzed reaction of the highly reactive BPL, BBL, and DIK is unfavored by their low basicity and occluded by their fast neutral hydrolysis. Thus, catalysis by hydronium ions cannot be observed at acid concentrations with $H_0 > -1$, which is equivalent to 20% sulfuric acid.[26−28,39] At these high acid concentrations, the activity of water is significantly decreased ($a_{H_2O} < 0.75$), which doubly disfavors the $A_{AC}2$ mechanism.

Our results suggest that at low concentrations of acid, in which the acid-catalyzed reaction is occluded by the neutral mechanism and cannot be observed experimentally, bimolecular hydrolysis is similarly rapid or even faster than unimolecular cleavage. However, under the experimental conditions (concentrated mineral acid), the barrier for $A_{AC}2$ is increased, and the kinetic parameters measured correspond to the now major $A_{AC}1$ pathway.

In order to model these empirical observations, the energy barriers were calculated for the pertinent mechanisms in the nearly complete absence and total absence of explicit solvent molecules.

3.6.1. One Explicit Water Molecule. Table 7 shows (i) the calculated activation free energies when one extra water molecule is included, for a total of one water molecule for unimolecular reactions and two water molecules (nucleophile plus catalyst) for bimolecular pathways and (ii) the results obtained when only the absolutely essential water molecules are included (one for bimolecular mechanisms, none for unimolecular ones). The self-consistent reaction field PCM solvation is maintained in all calculations.

In the intermediate situation, the primary and secondary β-lactones have clearly switched to the unimolecular pathway, midsized lactones now showing similar barriers for $A_{AC}2$ and $A_{AC}1$ and the linear esters still maintaining the $A_{AC}2$.

3.6.2. No Explicit Solvent. When only the strictly necessary water molecules are present, the situation changes further. The acidic tetrahedral intermediate in the $A_{AC}2$ mechanism is so high in energy and so far behind such a towering energy barrier that for all the molecules studied (with the obvious exception of tertiary BIVL), the $A_{AC}1$ mechanism is the lowest-energy reaction pathway. The energy barrier for this pathway is nevertheless higher than that of *standard* well-solvated $A_{AC}2$ hydrolysis, in accordance with the experimentally observed lower reaction rate once the change in the mechanism has occurred. The barrier for the $A_{AC}2$ addition in the case of AcOEt is exceptionally favored, in comparison with the lactones, although still higher in energy than the $A_{AC}1$ transition state. This effect could be related to the favored *trans* configuration of the ester bond.

Thus, the change from the bimolecular to the unimolecular acyl cleavage mechanisms can be interpreted as being influenced by exogenous and endogenous parameters: solvation and ring strain, respectively. If the activity of water is lowered, the availability of the $A_{AC}2$ mechanism decreases. Also, the presence of a strained ring increases the tendency of the lactones to undergo unimolecular ring-cleavage. Accordingly, the acid-catalyzed hydrolysis of BPL, BBL, and DIK can be seen as an extreme version of this trend, in which the decrease in water activity necessary for the change in the mechanism takes place at very low acid concentrations. Since DIK is the most reactive β-lactone, it is also the one showing the largest unimolecular contribution. On the opposite side are AcOEt, which requires very high concentrations of acid before the $A_{AC}1$ mechanism can be observed, and COOMe, for which the formation of the $A_{AC}1$ transition state is highly disfavored under all conditions because of the lack of substituents than could stabilize the acyl cation.

4. CONCLUSIONS

The various possible mechanisms of the acid-catalyzed hydrolysis of lactones have been modeled using density functional theory and a hybrid supermolecule−PCM approach. Good qualitative and quantitative agreement with experimental results in the literature has been found for a wide range of substrates and mechanisms, confirming the predicting ability of this approach.

The present results help us to understand the balance between the unimolecular ($A_{AC}1$) and bimolecular ($A_{AC}2$) reaction pathways. In contrast to the experimental setting, where one of the two branches is often occluded by the requirement of rather extreme experimental conditions, we have been able to estimate both contributions for all the compounds studied and found that they undergo a transition from $A_{AC}2$ to $A_{AC}1$ hydrolysis as acidity increases. The intrinsically more reactive β-lactones are more refractory to acid hydrolysis, and thus the $A_{AC}2$ region cannot be measured in kinetic experiments since it is occluded by the faster neutral hydrolysis. As intrinsic reactivity decreases (e.g., the larger lactones), the transition zone moves to higher acidities and can be detected in kinetic experiments by modifying the experimental conditions.

In addition, it has been found that protonated esters within an explicit solvation shell are not minima in their respective potential energy surfaces at the present levels of theory. This

dx.doi.org/10.1021/jo4002596 | J. Org. Chem. 2013, 78, 6880−6889

finding, and especially its relationship with the nature of the pre-equilibrium protonation reaction as a function of water activity, should help guide future experiments and theoretical work.

■ ASSOCIATED CONTENT

Supporting Information

Equilibrium geometries and energies for all computed structures, results at the MP2/6-31++G(d,p), MP4/6-31++G(d,p), and QCISD/6-31++G(d,p) levels of theory on B3LYP/6-31++G(d,p) geometries and also at the B3LYP/6-311++G(2df,pd) level of theory, $\Delta\Delta S_{solv}$ correction to enthalpies, and SCF energies and geometries used in pK_a calculations. This material is available free of charge via the Internet at http://pubs.acs.org.

■ AUTHOR INFORMATION

Corresponding Author

*E-mail: jucali@usal.es. Phone: +34 923 294486. Fax: +34 923 294574.

Notes

The authors declare no competing financial interest.

■ ACKNOWLEDGMENTS

The authors thank the Spanish Ministerio de Ciencia e Innovación and European Regional Development Fund (Project CTQ2010-18999) for supporting the research reported in this article. R.G.B. thanks the Spanish Ministerio de Educación for a Ph.D. grant (AP2006-01976). M. González-Pérez is acknowledged for her helpful discussion of the manuscript. We also thank the anonymous reviewers for their valuable comments.

■ REFERENCES

(1) Yamabe, S.; Fukuda, T.; Ishii, M. *Theor. Chem. Acc.* **2011**, *130*, 429−438.
(2) Zahn, D. *J. Phys. Chem. B* **2003**, *107*, 12303−12306.
(3) Wang, B.; Cao, Z. *J. Phys. Chem. A* **2010**, *114*, 12918−12927.
(4) Pan, B.; Ricci, M. S.; Trout, B. L. *J. Phys. Chem. B* **2011**, *115*, 5958−5970.
(5) Ingold, C. K. *Structure and Mechanism in Organic Chemistry*, 2nd ed.; Cornell University Press: Ithaca, NY, 1969; pp 457−463.
(6) Kirby, A. J. In *Ester Formation and Hydrolysis and Related Reactions*; Bamford, C. H., Tipper, C. F. H., Eds.; Comprehensive Chemical Kinetics; Elsevier: Amsterdam, The Netherlands, 1972; Vol. *10*, pp 57−201.
(7) McClelland, R. A. *J. Am. Chem. Soc.* **1974**, *97*, 3177−3181.
(8) Moore, J. A.; Schwab, J. M. *Tetrahedron Lett.* **1991**, *32*, 2331−2334.
(9) Wang, B.; Cao, Z. *Angew. Chem., Int. Ed.* **2011**, *50*, 3266−3270.
(10) Frisch, M. J.; Trucks, G. W.; Schlegel, H. B.; Scuseria, G. E.; Robb, M. A.; Cheeseman, J. R.; Scalmani, G.; Barone, V.; Mennucci, B.; Petersson, G. A.; Nakatsuji, H.; Caricato, M.; Li, X.; Hratchian, H. P.; Izmaylov, A. F.; Bloino, J.; Zheng, G.; Sonnenberg, J. L.; Hada, M.; Ehara, M.; Toyota, K.; Fukuda, R.; Hasegawa, J.; Ishida, M.; Nakajima, T.; Honda, Y.; Kitao, O.; Nakai, H.; Vreven, T.; Montgomery, J. A., Jr.; Peralta, J. E.; Ogliaro, F.; Bearpark, M.; Heyd, J. J.; Brothers, E.; Kudin, K. N.; Staroverov, V. N.; Kobayashi, R.; Normand, J.; Raghavachari, K.; Rendell, A.; Burant, J. C.; Iyengar, S. S.; Tomasi, J.; Cossi, M.; Rega, N.; Millam, J. M.; Klene, M.; Knox, J. E.; Cross, J. B.; Bakken, V.; Adamo, C.; Jaramillo, J.; Gomperts, R.; Stratmann, R. E.; Yazyev, O.; Austin, A. J.; Cammi, R.; Pomelli, C.; Ochterski, J. W.; Martin, R. L.; Morokuma, K.; Zakrzewski, V. G.; Voth, G. A.; Salvador, P.; Dannenberg, J. J.; Dapprich, S.; Daniels, A. D.; Farkas, O.; Foresman, J. B.; Ortiz, J. V.; Cioslowski, J.; Fox, D. J. *Gaussian 09*; Gaussian, Inc.: Wallingford, CT, 2009.
(11) Pliego, J. R.; Riveros, J. M. *J. Phys. Chem. A* **2001**, *105*, 7241−7247.
(12) Marenich, A. V.; Cramer, C. J.; Truhlar, D. G. *J. Phys. Chem. B* **2009**, *113*, 6378−6396.
(13) Fernández, D. P.; Goodwin, A. R. H.; Sengers, J. M. H. L. *Int. J. Thermophys.* **1995**, *16*, 929−955.
(14) Ho, J. M.; Coote, M. L. *Theor. Chem. Acc.* **2010**, *125*, 3−21.
(15) Liptak, M. D.; Shields, G. C. *J. Am. Chem. Soc.* **2001**, *123*, 7314−7319.
(16) Tissandier, M.; Cowen, K.; W.Y., F.; Gundlach, E.; Cohen, M.; Earhart, A.; Coe, J.; Tutle, T. *J. Phys. Chem. A* **1998**, *102*, 7787−7794.
(17) Camaioni, D.; Schwerdtfeger, C. *J. Phys. Chem. A* **2005**, *109*, 10795−10797.
(18) Kelly, C. P.; Cramer, C. J.; Truhlar, D. G. *J. Phys. Chem. B* **2006**, *110*, 16066−16081.
(19) Casasnovas, R.; Fernández, D.; Ortega-Castro, J.; Frau, J.; Donoso, J.; Muñoz, F. *Theor. Chem. Acc.* **2011**, *130*, 1−13.
(20) Bagno, A.; Lucchini, V.; Scorrano, G. *J. Phys. Chem.* **1991**, *95*, 345−352.
(21) Montgomery, J. A.; Frisch, M. J.; Ochterski, J. W.; Petersson, G. A. *J. Chem. Phys.* **1999**, *110*, 2822−2827.
(22) Montgomery, J. A.; Frisch, M. J.; Ochterski, J. W.; Petersson, G. A. *J. Chem. Phys.* **2000**, *112*, 6532−6542.
(23) Gómez-Bombarelli, R.; González-Pérez, M.; Pérez-Prior, M. T.; Calle, E.; Casado, J. *J. Org. Chem.* **2009**, *74*, 4943−4948.
(24) Bell, R.; Dowding, A.; Noble, J. *J. Chem. Soc.* **1955**, 3106−3110.
(25) Yates, K.; McClelland, R. A. *J. Am. Chem. Soc.* **1967**, *89*, 2686−2692.
(26) Long, F. A.; Purchase, M. *J. Am. Chem. Soc.* **1950**, *72*, 3267−3273.
(27) Olson, A. R.; Hyde, J. L. *J. Am. Chem. Soc.* **1941**, *63*, 2459−2461.
(28) Olson, A. R.; Miller, R. J. *J. Am. Chem. Soc.* **1938**, *60*, 2687−2692.
(29) Briody, J. M.; Satchell, D. P. *J. Chem. Soc., Chem. Commun.* **1965**, 3778−3785.
(30) Lee, D. G.; Sadar, M. H. *J. Am. Chem. Soc.* **1974**, *96*, 2862−2867.
(31) Lane, C. A. *J. Am. Chem. Soc.* **1964**, *86*, 2521−2523.
(32) Lane, C. A.; Cheung, M. F.; Dorsey, G. F. *J. Am. Chem. Soc.* **1968**, *90*, 6492−6494.
(33) Bordejé, M. C.; Mó, O.; Yáñez, M.; Herreros, M.; Abboud, J. L. M. *J. Am. Chem. Soc.* **1993**, *115*, 7389−7396.
(34) Pérez-Prior, M. T.; Manso, J. A.; García-Santos, M. P.; Calle, E.; Casado, J. *J. Org. Chem.* **2005**, *70*, 420−426.
(35) Tommila, E.; Murto, M. *Acta Chem. Scand.* **1963**, *17*, 1957−1970.
(36) Liang, H. T.; Bartlett, P. D. *J. Am. Chem. Soc.* **1958**, *80*, 3585−3590.
(37) Boer, F. P. *J. Am. Chem. Soc.* **1968**, *90*, 6706−6710.
(38) Chevrier, B.; Le Carpentier, J. M.; Weiss, R. *J. Am. Chem. Soc.* **1972**, *94*, 5718−5723.
(39) Bartlett, P. D.; Rylander, P. N. *J. Am. Chem. Soc.* **1951**, *73*, 4273−4274.